LITERATURE CITED

AIChE, "Bubble Tray Design Manual, Prediction of Fractionation Efficiency," *AIChE*, New York (1958).

Bell, R. L., "Experimental Determination of Residence Time Distributions on Commercial Scale Distillation Trays using a Fiber Optic Technique," *AIChE J.*, **18**, 491 (1972a).

———., "Residence Time and Fluid Mixing on Commercial Scale Sieve Trays," *ibid.*, **18**, 498 (1972b).

Crozier, R. S., Ph.D. thesis, Univ. of Michigan, Ann Arbor (1955).

Foss, A. S., J. A. Gerster, R. L. Pigford, "Effect of Liquid Mixing on the Performance of Bubble Trays," *AIChE J.*, **4**, 231 (1958).

Gerster, J. A., A. B. Hill, N. N. Hochgraf, D. B. Robinson, "Tray Efficiencies in Distillation Columns," Final Report, Univ. of Delaware, Newark (1958).

Keller, G. J., and T. Yanagi, Film, "Fluid Flow on Fractionation Trays," paper presented at AIChE 68th National Meeting (1970).

Lebedev, Y. N., I. A. Aleksandrov, and D. D. Zykov, "Combined Hydrodynamic Models of Fractionating Column Trays under Crossflow Conditions," *Teor. Osnovy Khim. Tekhno.*, **2**, 2, 183 (1968).

Lewis, W. K., "Rectification of Binary Mixtures. Plate Efficiency of Bubble Cap Columns," *Ind. Eng. Chem.*, **28**, 399 (1936).

Oliver, E. D. and C. C. Watson, "Correlation of Bubble-Cap Fractionating-Column Plate Efficiencies," *AIChE J.*, **2**, 18 (1956).

Porter, K. E., M. J. Lockett, and C. T. Lim, "The Effect of Liquid Channeling on Distillation Plate Efficiency," *Trans. Instn. Chem. Engrs.*, **50**, 91 (1972).

Strand, C. P., "A New Look at Distillation.—Bubble Cap Tray Efficiencies," *Chem. Eng. Progr.*, **59**, 58 (1963).

Warzell, L., Ph.D. thesis, Univ. of Michigan, Ann Arbor (1955).

Williams, B., J. W. Begley, and C. Wu, "Tray Efficiencies in Distillation Columns." AIChE Research Committee, Univ. of Michigan Final Report (1960).

Yanagi, T., and B. D. Scott, "Effect of Liquid Mixing on Sieve Trays," *Chem. Eng. Progr.*, **69**, 75 (1973).

Manuscript received August 18, 1972; revision received March 12 and accepted March 13, 1974.

Statistical Characteristics of Thin, Wavy Films:

Part II. Studies of the Substrate and its Wave Structure

Waves on falling liquid films display certain random features. At least two classes of such random waves are shown to exist; large waves which carry the bulk of the fluid and small waves which cover a substrate film that exists between large waves. It is shown that the statistics of the substrate thickness and its wave structure can be extracted from measurements of the variation of film thickness with time. A theory is presented for calculating the mean substrate thickness and the substrate flow rate. The statistics of the wave structure is presented and compared with existing theory. The importance of the substrate in controlling transfer processes is demonstrated.

K. J. CHU
and
A. E. DUKLER

Chemical Engineering Department
University of Houston
Houston, Texas 77004

SCOPE

The flow of thin liquid films occurs in a wide variety of process equipment including falling film evaporators, reactors and wetted wall towers, thermosyphon reboilers, direct fired tubular boilers, and pipeline reactors. Experimental observations have shown that in almost all cases of practical interest the liquid displays random waves at the interface and that rates of transfer of heat and mass are greatly enhanced by the presence of these waves (Dukler, 1972). The use of simple transport equations and the assumption of a smooth interface fail to describe the process accurately and, as a result, the reliability of design procedures for such process equipment has been inadequate (Alves, 1970). Improving design procedures for thin, wavy film systems requires information on the wave structure and the manner in which the waves change the velocity fields in the liquid and gas phases bounded by the interface. But the wave structure has been shown to be a complex one. There appear to be several classes of waves and each class has certain random features. In particular, it is already known (Telles and Dukler, 1970) that the interface consists of waves large in amplitude compared to the film thickness which are separated by a very thin liquid substrate, itself covered by small waves. The substrate plays an important role in determining transport of heat and mass through the film. The purpose of this paper is to present new methods for extracting the meaningful statistical information about the substrate and its wave structure and to interpret the results of a very detailed study of that substrate under a variety of conditions of flow and shear. This hydrodynamic data can then provide the information needed to model the transfer processes. A subsequent paper in the series will discuss the large wave structure.

CONCLUSIONS AND SIGNIFICANCE

New data on the statistics of the substrate and its associated wave structure are presented for a wide range of liquid and gas rates covering flow situations of importance in film flow type process equipment. A method of time series analyses is presented which permits the statistics of the substrate to be extracted from the statis-

Correspondence concerning this paper should be addressed to A. E. Dukler.

tics of the film thickness. The technique is applicable to other systems where the characteristics of one random process must be determined from a signal which is caused by two random processes. The substrate is shown to be present for a large fraction of the time (Figure 11) even though only a small fraction of the liquid flows in the substrate (Figure 12). Thus the substrate has a very strong influence on the transfer of heat or mass into the film.

A theory is developed for the average substrate film thickness given the celerity of the large waves. Since the wave structure on the substrate depends on the film thickness, it is clear that the structure of the small and large waves are coupled through this celerity. Agreement with data is good (Figure 14).

Probability densities for amplitude and length of substrate waves show a unimodal character with little or no dependence on gas rate (interfacial shear). This is in contrast with the observed strong dependence of the large wave structure on gas flow. Even at very high film flow rates the substrate Reynolds number is low and the wave amplitude and slope are small. Most published theories for prediction of wave amplitude, length, and celerity require these conditions. Thus, for the first time such theories can be tested in a definitive way. Surprisingly, none of these theories does a satisfactory job of predicting these properties (Figures 18, 21 to 23). The data show that even these small substrate waves are highly nonsymmetrical. All extant theories depend for their success on a description of the wave with only a few terms in a Fourier series, and it is now evident that this can not describe the observed waves. Wave shape and size are important to the prediction of heat and mass transfer in the substrate and this indicates that a new approach is needed.

Experimental studies of the structure of thin, vertical falling films have demonstrated the random nature of the interface (for example, Telles and Dukler, 1970; Webb, 1970; Wicks, 1967). This randomness has been represented by the probability distribution or the spectral density of the film thickness; but this provides little of the needed information about the structure of the waves. Telles and Dukler (1970) in the first paper of this series showed that the gas-liquid interface can be represented by a two wave system. Large lumps of liquid, which carry a significant portion of all flowing liquid, move down the interface with essentially constant shape and speed. A smaller wave structure exists over the substrate, as well as across the large waves. As an initial approach to extracting information about wave structure from the statistics of the film thickness, they treated all large waves as being of a single size and shape moving across a smooth substrate. The observed randomness of the film thickness was attributed to random separation distances between these large waves. With this model it was possible to calculate the size and shape of the large waves from the measured probability and spectral density of the film thickness. Essentially, that approach assumed that the statistics of the film thickness is dominated by the large waves.

Some typical film thickness traces obtained in this study are shown in Figure 1. These traces reveal (1) the substrate is not smooth, (2) the amplitude of all large waves is not constant, (3) in addition to the class of small waves which cover the substrate there exists a different small wave structure which rides on the large waves, and (4) the statistics of the film thickness are significantly influenced by the substrate and its waviness.

The existence of separate small and large wave structures as described above leads one to believe that the physics controlling each of these types are likely to be quite different. The present state of mathematical tools is insufficient to describe the entire wave system in one complete model. Thus, it is useful to calculate the statistics of each wave type separately to provide information for development of separate models for each class of waves. This paper is concerned with the substrate and its wave structure.

Measurements treating the film thickness as a random process are relatively recent developments. Limited studies by Wicks (1967), Telles (1968), and Webb (1970) have been made to obtain such measurements. But there has been no attempt to extract the statistical information on the substrate structure from those film thickness measurements. Observations of many film thickness traces shows that at any fixed point along a surface the substrate is present for a large fraction of the time. It therefore plays an important role in the processes of transfer which take place between the wall and liquid or between phases.

The purpose of this paper is to present information on this substrate structure and to interpret these data. Future papers will consider the large wave structure in more detail. Two groups of statistical parameters are used here: one considers the film thickness of the substrate as a random process and another considers the individual small waves on the substrate as a random process. A theoretical prediction of mean film thickness of the substrate from a single large wave parameter the celerity C, is also given. Detailed data are presented by Chu (1973).

EXPERIMENTAL EQUIPMENT

The flow system consisted of a 4.27-m long vertical test section with four measuring stations, a 1.22-m long air-water entry section and a 0.61 m long air-water separation section. A schematic flow diagram of the system is given in Figure 2.

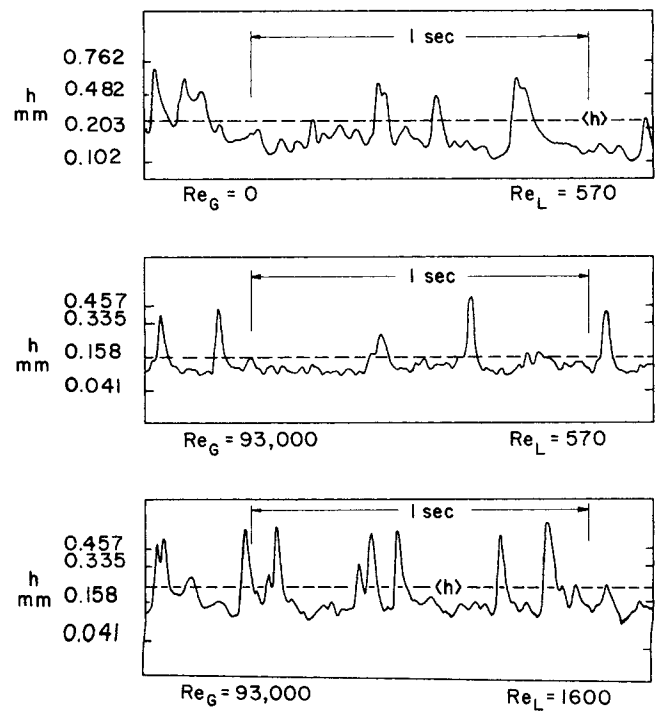

Fig. 1. Typical film thickness traces.

The test section was made of 4 lengths of 5.080 ± 0.005-cm I.D. Plexiglass pipe with lengths of 0.305 m, 0.610 m, 1.220 m, and 1.830 m. Each length was fitted with special flanges having an interlocking O ring constructed to match a measuring station with no internal discontinuity. There were four measuring stations, each located between two adjacent test section lengths. Each individual station consisted of four pairs of conductivity probes for film thickness measurement and four pressure channels to measure instantaneous pressure, located at 90° intervals around the circumference. A detailed sketch of this system is given in Figure 3. The conductivity probes are similar to those developed in this laboratory by Wicks (1967) and Telles (1968) for the study of film thickness on flat plates. The electrodes were made of silver foil, 0.051 mm in thickness, and were carefully platinized to insure stable performance.

In order to obtain reliable data on the small scale wave structures, it was necessary to evolve a scheme for collecting and processing the time series data in a way to prevent small errors. This procedure is discussed in detail by Chu (1973). In summary, the following scheme was used: An AC voltage with 1 KC frequency and constant amplitude was applied to each electrode pair. The current which passed through the liquid varied with the local film thickness and this variation was measured by detecting the voltage drop across a standard resistor. The signal carried a one KC oscillation whose amplitude varied as the film thickness changed. The 1 KC fluctuation was removed by passing the signal through linear full wave rectifiers and low pass filters to produce a D.C. signal whose instantaneous amplitude was related to the instantaneous film thickness and this information was stored on one channel of analog tape as a voltage variation with time. Signals from all stations were simultaneously recorded. Data processing was accomplished digitally by passing the voltage signal from each channel of the tape through an A/D converter to an IBM 360-44 core storage where calibration and corrections were applied to each point. The resulting film thickness sequence for discrete points in time was stored on magnetic tape for subsequent data processing.

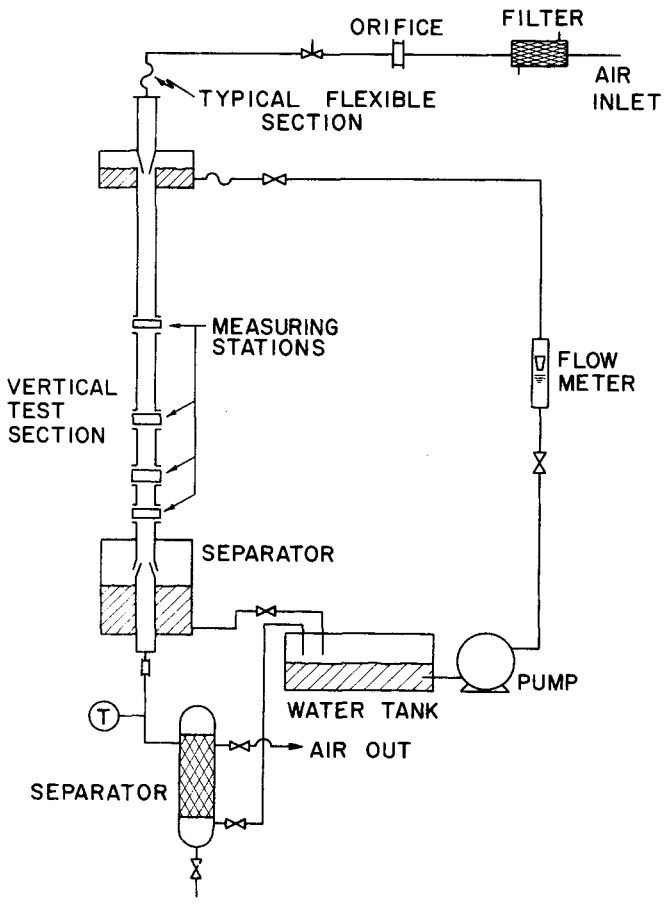

Fig. 2. Flow loop.

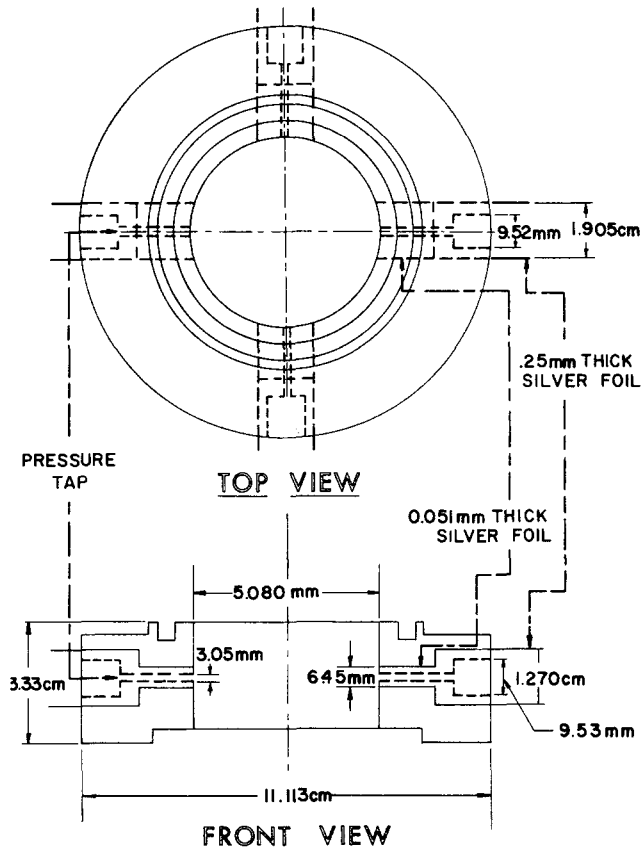

Fig. 3. Film thickness measuring station.

A sequence of calibrations and corrections were used to accurately convert the voltage signal to film thickness. The cell constant for each electrode pair in each measuring station was determined as a function of film thickness in an apparatus external to the system. Liquid films of known thickness were created by flowing water through annular gaps which were formed by using the measuring station (Figure 3) as the outer wall and positioning a series of plastic inserts of diameters smaller than 5.08 cm at the axis. A Leeds and Northrup precision conductivity bridge was used along with a standard conductivity cell. The cell constant is, of course, independent of temperature or salinity of the water.

The electronic conductivity monitoring circuit was calibrated with a precision decade resistance box. Compensation for possible errors due to drift or electronics in the analog tape recorder or the analog to digital conversion equipment was accomplished by simultaneously recording on separate channels a known voltage drop across two standard resistors selected so as to bracket the highest and lowest voltages recorded for the film thickness signals. The voltages were compared after playback and digitation and a linear transformation used to correct all digitized data. Conductivity of the water was continuously monitored by passing part of the liquid leaving the test section through a standard cell. Film thickness from conductivity probes is a nonlinear function of the measured cell voltage. In all previous published studies, statistical analysis was always carried out on the voltage trace, making conclusions as to film properties somewhat ambiguous. In this work the analysis is carried out on the film thickness trace (after conversion from voltage to film thickness using the calibration curve) and the ambiguity is completely eliminated. The accuracy of the time series, $h(t)$, is 0.0254 mm in the amplitude domain and 0.004 in the time domain.

DATA PROCESSING

Substrate and Its Small Waves

In order to calculate the statistics of the substrate and its small waves from the time series, $h(t)$, it is necessary

to establish the criteria for identifying small and large waves. The words, *large waves*, imply that a large fluctuation takes place about the mean film thickness with the minimum and maximum film thickness associated with the wave being on alternate sides of the mean. In an analogous way, small waves on the substrate appear to be completely below the mean film thickness. In fact, three classes of waves can be identified as follows:

1. A large wave exists if an excursion in film thickness is found such that:

$$h_{max} > \langle h \rangle \text{ and } h_{min},\ h'_{min} < \langle h \rangle$$

2. A small wave exists on the substrate if for that excursion,

$$h_{max},\ h_{min},\ h'_{min} < \langle h \rangle$$

3. A small wave exists on large waves if one of three possible conditions are detected:

$$h_{max} > \langle h \rangle,\quad h_{min} > \langle h \rangle,\quad h'_{min} < \langle h \rangle$$
$$h_{max} > \langle h \rangle,\quad h_{min} < \langle h \rangle,\quad h'_{min} > \langle h \rangle$$
$$h_{max} > \langle h \rangle,\quad h_{min} > \langle h \rangle,\quad h'_{min} > \langle h \rangle$$

where

$\langle h \rangle$ is the mean film thickness
h_{max} is the film thickness at the crest of the wave
h_{min} is the film thickness at the trough in front of the wave
h'_{min} is the film thickness at the trough in back of the wave

In all previous studies the substrate thickness was defined as that thickness below which the probability density of the film thickness is zero and above which the probability density is nonzero. Physically this definition implies that there exists a smooth continuous substrate film of liquid between two consecutive large wave peaks. But the data in this study show that small waves ride on the substrate and, in the time domain, the number of small waves is over twice that of the large waves. In this study, the substrate thickness $h_s(t)$ is defined as the portion of film thickness which is covered by small waves such that h_{max}, h_{min}, $h'_{min} < \langle h \rangle$. Figure 4 illustrates these ideas and also compares some properties of large and small waves which were measured at one Reynolds number. The drastic difference in properties between these two classes of waves is apparent.

Probability Density of Substrate Thickness $h_s(t)$

The data show that the amplitude of the small waves fluctuates within a narrow range. Thus the contribution of $h_s(t)$ to the probability density function of $h(t)$ shows a modal peak around the mean values of $\langle h_s \rangle$. The amplitude of these waves is quite small and the wave slope in the time domain is essentially linear. Then the probability density function of h_s should be symmetrical around $\langle h_s \rangle$, a value roughly equal to the modal value of $\tilde{f}(h)$. Based on these ideas, the probability density function for the thickness of the substrate $\tilde{f}\hat{}_{h_s}(h_s)$ can be extracted from that of the film $\tilde{f}\hat{}_h(h)$ by the following procedures:

1. The probability density function $\tilde{f}\hat{}_h(h)$ can be represented as the curve *abcdefghijk* in Figure 5.

2. Since $\tilde{f}\hat{}_{h_s}(h_s)$ is symmetrical about $\langle h_s \rangle$ in the neighborhood of $\langle h_s \rangle$ and $\langle h_s \rangle$ is approximately equal the modal value of $\tilde{f}\hat{}_h(h)$, then one obtains the point f', g', h' for the substrate by setting them equal to d, c, b.

3. Taking the difference between pairs of (f, f'), (g, g') and (h, h'), the curve f'', g'', h'', which represents the contribution of the large waves is determined.

4. Extrapolating the curve f'', g'', h'' to point a, one obtains the curve b'', c'', d'' and e'' for the large waves. Subtracting this curve from b, c, d, e, the curve b', c', d' and e' for the substrate is calculated. Call these two curves $\tilde{CV}_s$ and $\tilde{CV}_w$, respectively. Then

$$F_s = \int_0^\infty \tilde{CV}_s\, dh \tag{1}$$

$$F_w = \int_0^\infty \tilde{CV}_w\, dh \tag{2}$$

$$\tilde{f}\hat{}_{h_s}(h_s) = \tilde{CV}_s / F_s \tag{3}$$

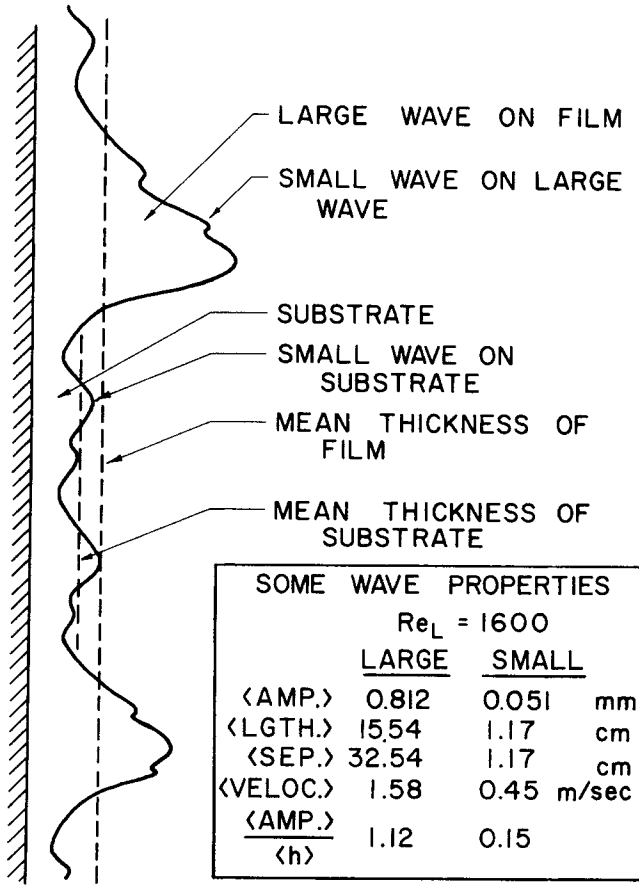

SOME WAVE PROPERTIES
Re_L = 1600

	LARGE	SMALL	
⟨AMP.⟩	0.812	0.051	mm
⟨LGTH.⟩	15.54	1.17	cm
⟨SEP.⟩	32.54	1.17	cm
⟨VELOC.⟩	1.58	0.45	m/sec
⟨AMP.⟩/⟨h⟩	1.12	0.15	

Fig. 4. Identification of wave class.

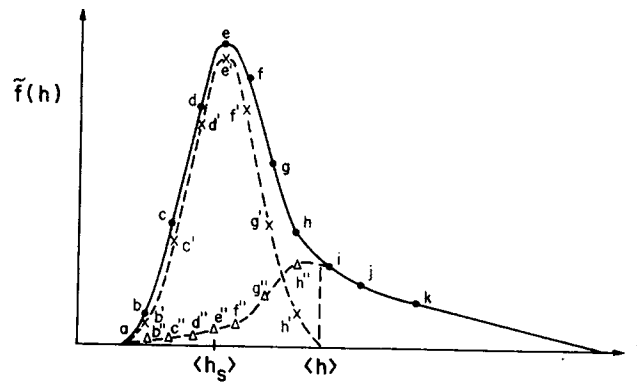

Fig. 5. Extracting the probability density of the substrate.

$$\tilde{f}_{\hat{h}\,w}(h_w) \simeq \tilde{C}V_w/F_w \qquad (4)$$

where

F_s = the time fraction substrate is observed passing a fixed point in space

F_w = the time fraction large waves pass a fixed point in space

$\tilde{f}_{\hat{h}\,w}$ = the probability density function of the film thickness during passage of large waves and the small waves on the large waves

$\tilde{f}_{\hat{h}\,s}$ = the probability density function for the substrate thickness.

The result of such a decomposition for one flow condition appears in Figure 6.

Probability Density of Wave Parameters

Previous reports except that of Telles and Dukler (1970) assume the waves on falling films are sinusoidal and can thus be completely specified by three parameters: wave amplitude A, and two of three parameters; wave length, λ, wave period T, and wave velocity c. But it is now clear that sinusoidal waves never occur on a falling film under flow conditions of practical interest. In this study the waves are considered as nonsymmetrical and measured in terms of two types of parameters: one measured in the time scale to characterize the base dimensions of the wave and one measured in the length scale to characterize amplitude. A length scale for the base can be obtained once the wave velocity c has been determined. In the time domain, the wave parameters of interest are time for passage of the base of the wave T_{bs}, wave separation time T_{sep}, time for passage of the wave front T_{fn}, and time for passage of back of the wave T_{bk}. Separation time between large waves differs from the base dimensions because of the existence of numerous small waves on the substrate between two successive large waves. In the amplitude domain, the wave parameters of interest are amplitude A and film thickness at the minimum of the wave. Because the minimum film thickness in front and in back of a wave are not necessarily the same, the definition of wave amplitude is

$$2A = h_{\max} - (h_{\min} + h'_{\min})/2 \qquad (5)$$

Calculation of the statistical properties of these seven parameters for each of the three types of waves proceeds from the digitized data, h_i, with $i = 1, 3, \ldots n$, the time interval between successive points being $\Delta\tau = 1/f_D$, where f_D is the digitizing frequency. Software was developed which, given this sequence of discrete values of film thicknesses, h_i, would

1. Search for a maximum and minimum.
2. Calculate the time interval between successive $h_{\min}$ and $h_{\max}$.
3. Repeat this process and form a series, $h^j_{\min}$, T^j_{fn}, $h^j_{\max}$, T^j_{bk}.
4. Separate this series into three sub series, one for each class of waves according to the criteria discussed above.
5. Calculate the series, A^j, T^j_{bs}, T^j_{sep} for each wave class.
6. Calculate the probability density, mean and variance for each of the seven wave properties and each class of wave.

With this information the substrate time fraction F_s can be calculated,

$$F_s = \frac{N_s<T_{bs}>_s}{N_w<T_{sep}>_w} \qquad (6)$$

Velocity of Small Waves on the Substrate

An important wave parameter which is not directly obtainable from the time series analysis is the wave velocity c. Telles assumed that the film thickness observed at two positions, 1 and 2 along the flow path, are two stationary stochastic processes such that

$$\hat{h}_1'(t) = \hat{h}'\left(t - \frac{x}{c}\right) \quad \text{at} \quad x = 0 \qquad (7)$$

$$\hat{h}_2'(t) = \hat{h}'\left(t - \frac{x}{c}\right) \quad \text{at} \quad x = l \qquad (8)$$

where l is separation distance between the two position and $\hat{h}_i'(t) = \hat{h}_i(t) - <\hat{h}_i(t)>$, $i = 1, 2$. Then from the definition of spectrum and covariance function, one obtains

$$\tilde{C}_{12}(\tau) = <h'(t+\tau)\hat{h}'\left(t - \frac{l}{c}\right)> = \tilde{C}_{11}\left(\tau + \frac{l}{c}\right) \qquad (9)$$

$$\tilde{S}_{12}(f) = \int_{-\infty}^{+\infty} e^{-i2\pi f\tau}\tilde{C}_{11}\left(\tau + \frac{l}{c}\right)d\tau = \tilde{S}_{11}(f)\exp\left[i2\pi f\frac{l}{c}\right] \qquad (10)$$

$$\tilde{\Lambda}(f) = \tilde{S}_{11}(f)\cos 2\pi f\frac{l}{c} \qquad (11)$$

$$\tilde{Q}(f) = \tilde{S}_{11}(f)\sin 2\pi f\frac{l}{c} \qquad (12)$$

where $\tilde{C}_{11}(\tau)$ and $\tilde{C}_{12}(\tau)$ are auto- and cross-covariance functions, $\tilde{S}_{11}(f)$ and $\tilde{S}_{12}(f)$ are auto- and cross-spectrum, and $\tilde{\Lambda}(f)$ and $\tilde{Q}(f)$ are co and quadrature spectrum. Finally the phase spectrum can be calculated from Equations (11) and (12) as

$$\tilde{\theta}(f) = 2\pi f\frac{l}{c} \qquad (13)$$

Equation (13) implies that the slope of the phase spectrum (θ vs. f) is constant since it is equal to the ratio of

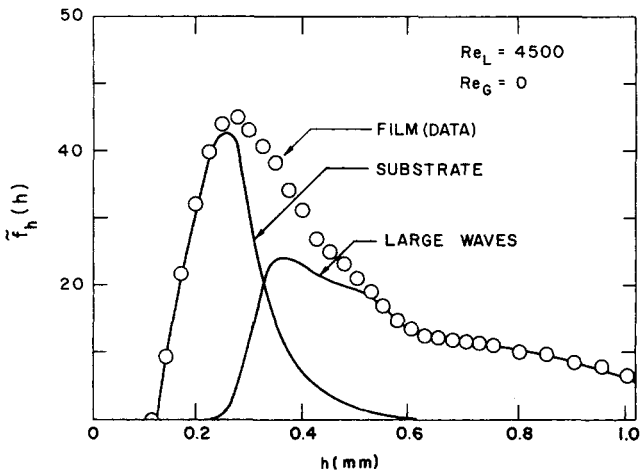

Fig. 6. Contribution of substrate and large waves to probability density of the film.

the fixed separation distance and the constant wave velocity c. The data for phase spectra in this work as well as that of Telles show a departure from the constant slope above a frequency of about 10 cps. The data also show that the large waves as defined here are always associated with frequencies below this value. Information on the celerity of the small waves can be developed by assuming that the process $\hat{h}(\tau)$ contains two components as discussed above, $\hat{h}_w'(t)$ and $\hat{h}_s'(t)$. $\hat{h}_w'(t)$ is moving at constant velocity c_w. $\hat{h}_s'(t)$ is moving at another velocity c_s. At the two measuring locations, 1 and 2, the observed signals would then be

$$\hat{h}_1'(t) = \hat{h}_w'\left(t - \frac{x}{c_w}\right) + \hat{h}_s'\left(t - \frac{x}{c_s}\right) \quad \text{at} \quad x = 0 \tag{14}$$

$$\hat{h}_2'(t) = \hat{h}_w'\left(t - \frac{x}{c_w}\right) + \hat{h}_s'\left(t - \frac{x}{c_s}\right) \quad \text{at} \quad x = l \tag{15}$$

$\hat{h}_w'(t)$ and $\hat{h}_s'(t)$ are uncorrelated and can be approximated by two Fourier sine series.

$$\hat{h}_w'\left(t - \frac{x}{c_w}\right) = \sum_{j=1}^{n} \hat{a}_j \sin \frac{2\pi}{T_j}\left(t - \frac{x}{c_w}\right) \tag{16}$$

$$\hat{h}_s'\left(t - \frac{x}{c_s}\right) = \sum_{j=k}^{m} \hat{b}_j \sin \frac{2\pi}{T_j}\left(t - \frac{x}{c_s}\right) \tag{17}$$

where $jT_j = T_1$ and $1 \leq k < n < m$. Then the phase spectrum would be

$$\theta_{12}(\omega) = \text{TAN}^{-1} \frac{\left\{ \sum_{j=1}^{n} \frac{\langle a_j^2 \rangle}{2} \pi \sin j\,\omega_1 \frac{l}{c_w} + \sum_{k}^{m} \frac{\langle b_j^2 \rangle}{2} \pi \sin j\,\omega_1 \frac{l}{c_s} \right\} \delta(j\omega_1 - \omega)}{\left\{ \sum_{j=1}^{n} \frac{\langle a_j^2 \rangle}{2} \pi \cos j\,\omega_1 \frac{l}{c_w} + \sum_{k}^{m} \frac{\langle b_j^2 \rangle}{2} \pi \cos j\,\omega_1 \frac{l}{c_s} \right\} \delta(j\omega_1 - \omega)} \tag{18}$$

$$\omega_1 = 2\pi/T_1$$

In the following two regions of frequency, one would have

$$\tilde{\theta}_{12}(w) = \begin{cases} j\omega_1 \dfrac{l}{c_w} & \text{for} \quad j = 1, \ldots, k-1 \\ j\omega_1 \dfrac{l}{c_s} & \text{for} \quad j = n+1, \ldots, m \end{cases} \tag{19}$$

Thus it has been shown that at low frequencies a linear phase angle with frequency is observed with slope related to the celerity of the large waves. At higher frequencies characteristic of the small waves a second linear region will be observed with the slope related to the constant celerity of the small waves. Then the wave velocity of small waves c_s can then be extracted from the phase spectrum in the range of small wave frequencies.

While the principle is clear, the fact that the large waves dominate the random process $\hat{h}(t)$ make the direct measurement of slope of the phase angle at high frequency an inaccurate one. To overcome this difficulty, a procedure was evolved to eliminate the influence of the large waves on the data by a time shift as follows: Designate $\tau_1 = l/c_w$ and shift the time series for film thickness at station 2 letting $\hat{h}_3'(t)$ be the shifted signal

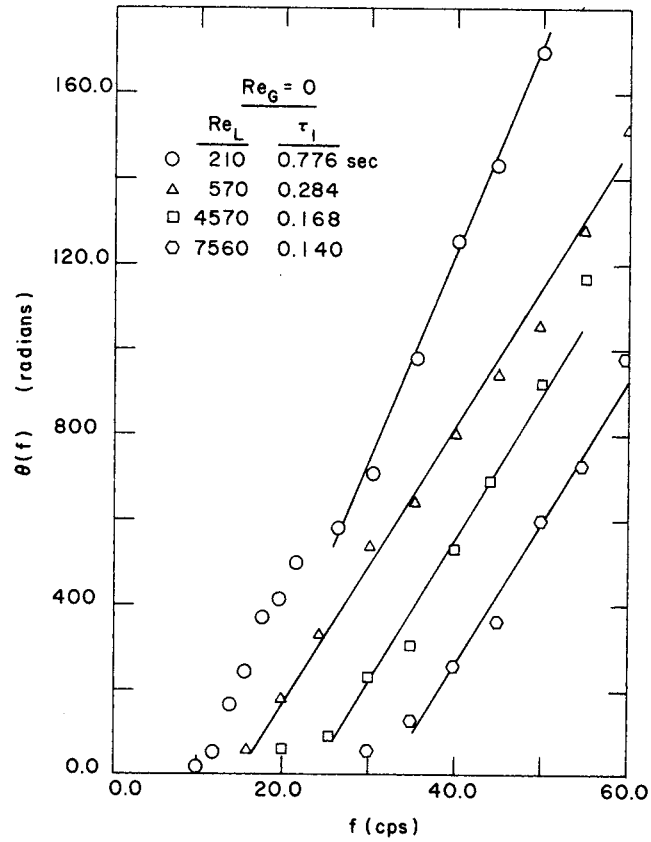

Fig. 7. Phase angle for small waves.

$$\hat{h}_3'(t) = \hat{h}_2'(t + \tau_1) \tag{20}$$

The phase spectrum $\theta_{13}(\omega)$ between the shifted signal at station 2 and the unshifted signal at 1 then is identical with Equation (18) with each l/c term in the sign terms replaced by $(l/c_w - \tau_1)$. But since $l/c_w - \tau_1 = 0$ and $\langle a_j^2 \rangle >> \langle b_j^2 \rangle$ (amplitude of large waves much greater than small waves) then

$$\theta_{13}(\omega) = 0 \qquad \text{for} \quad j = 1, \ldots, k-1$$

$$\theta_{13}(\omega) = j\omega_1\left(\frac{l}{c_s} - \tau_1\right) \quad \text{for} \quad j = n+1, \ldots, M \tag{21}$$

A typical phase spectrum obtained by this method is shown in Figure 7. The wave velocity c_s is thus extracted by setting the slope of these lines equal to $2\pi f(l/c_s - l/c_w)$. c_w is calculated from the slope of the unshifted signals at low frequency.

EXPERIMENTAL RESULTS

Substrate

Probability Density of Substrate. Probability density functions for the substrate as extracted from probability density of the film thickness for four liquid rates at zero gas flow rate appear in Figure 8 and for four gas rates at the same liquid flow rate are shown in Figure 9. From

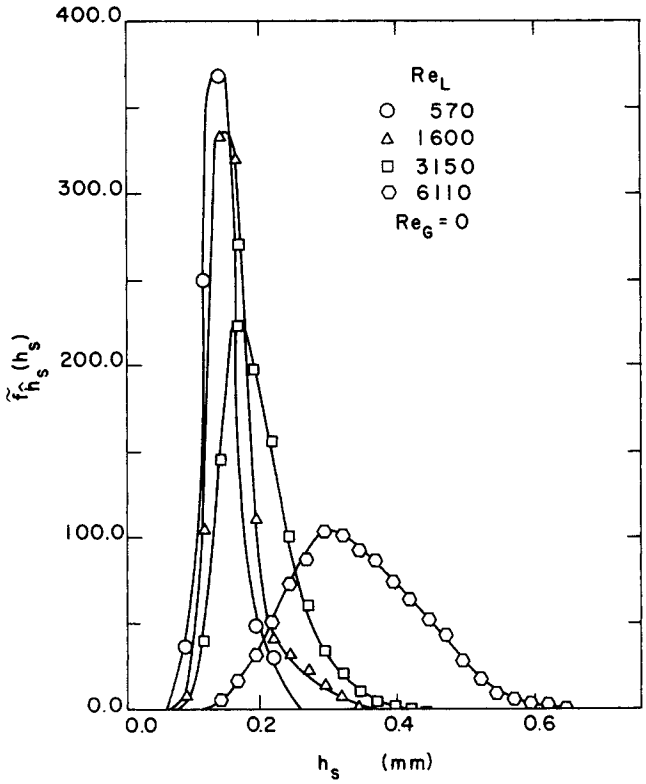

Fig. 8. Probability density of substrate thickness.

these data one can observe the following general characteristics: (1) The curve is roughly symmetrical around the modal value. (2) The maximum peak values decrease rapidly with decreasing liquid flow rate. The location of the modal value and the spread of the curve shows an inverse effect. (3) The gas flow rate has only a small effect on the maximum peak values, the modal value, or the spread of the curve. These observations indicate the substrate structure strongly dependent on the liquid flow rate and only slightly dependent on the gas. This situation differs drastically from that of the large wave structure.

Expected Value of Substrate Thickness $\langle h_s \rangle$. From the above probability densities it is possible to calculate the expected value of the substrate thickness:

$$\langle h_s \rangle = \int h_s \tilde{f}_{\hat{h}_s}(h_s) dh_s \qquad (22)$$

and these are shown in Figure 10.

Fractional Time of Exposure of Substrate, F_s. Data for F_s calculated using Equation (6) appears in Figure 11 for two gas rates. Results using Equation (1) give nearly identical values except at very low liquid rates. The quantity F_s is a secondary variable of the wavy system depending on the structure of the large waves. The data does show, that at liquid rates expected in process equipment, the substrate is exposed to the adjacent gas stream for 30 to 50% of the time. As will be shown, the mass carried by this substrate is small, and the process of transfer to such a wavy film system will depend strongly on the flow behavior of the substrate.

Substrate Flow. The widely separated large disturbance waves which travel rapidly across the substrate carry a substantial portion of the fluid introduced into the test section. With the information reported here on substrate properties, it is now possible to calculate the amount of liquid flowing in the substrate. Clearly, rather different gradients in velocity, concentration, or temperature can be expected in this thin, slow moving substrate than in the large wave portions of the film.

The local Reynolds number is a random process since the local flow rate varies with the local film thickness

$$\hat{Re}_L = \frac{4\hat{W}_L}{\pi D \mu_L} \qquad (23)$$

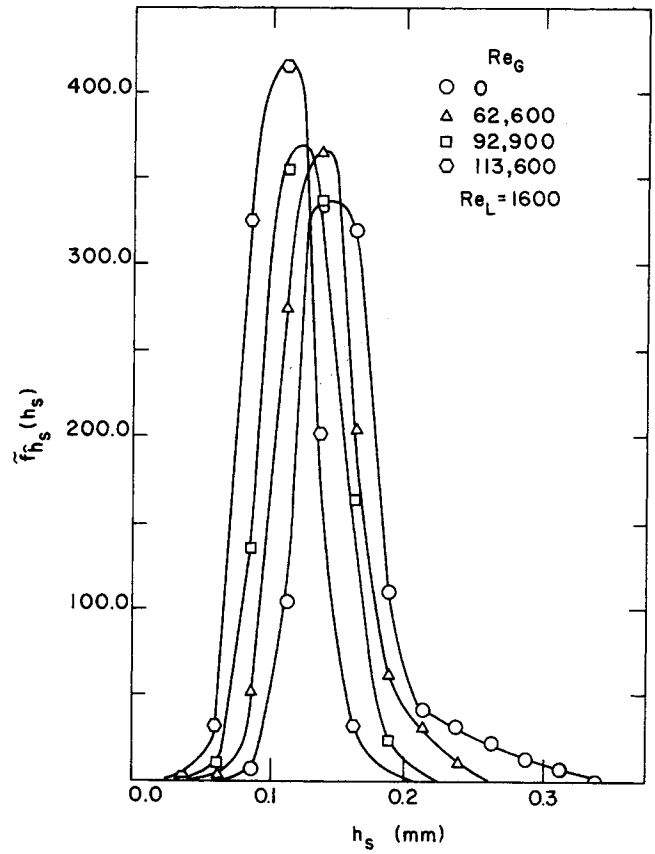

Fig. 9. Probability density of substrate thickness.

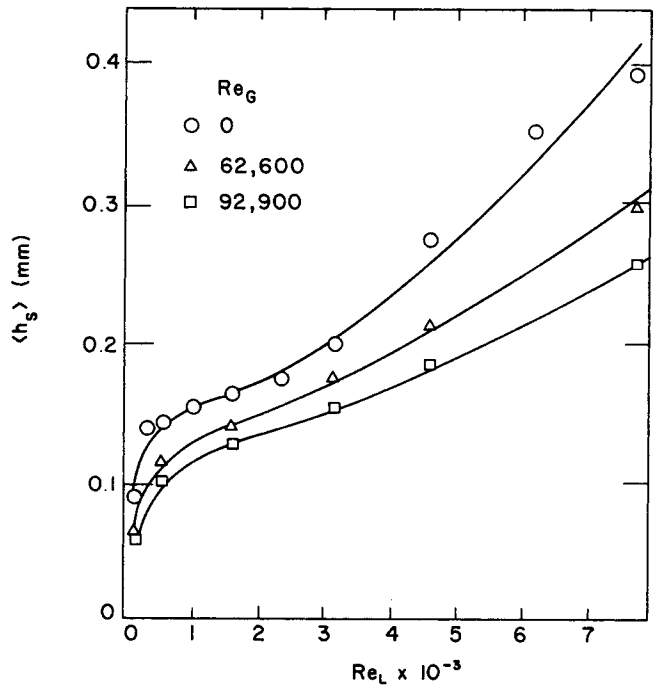

Fig. 10. Mean value of substrate thickness.

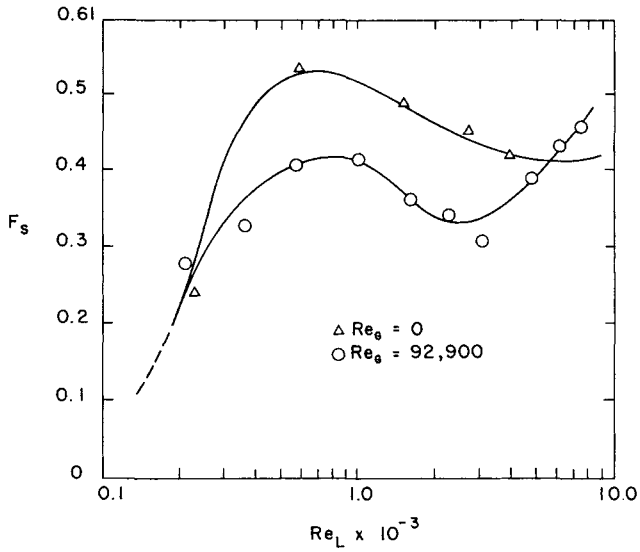

Fig. 11. Fractional exposure time for substrate.

The local Reynolds number averaged over the film length, or over large time must equal the Reynolds number based on the known rate of flow of liquid to the test section Re_L.

$$Re_L = \frac{4\rho_L}{\mu_L}\int_{-\infty}^{\infty}\left\{\int_0^{\hat{h}} u(y)dy\right\}\tilde{f}_{\hat{h}}(h)dh \quad (24)$$

In general, it is not possible to specify the velocity distribution for this integration since, in the presence of the large waves, the usual assumption of parallel flows ignores important acceleration terms (Chu, 1973). However, for the substrate the waves are small in amplitude and slope (see below) and these acceleration terms are small. It is thus possible to use the velocity distribution of Nusselt (1916) for laminar flow or Dukler (1959) for laminar or partially turbulent films with negligible error. Equation (24), restated for the substrate, is

$$\langle Re_s\rangle = \frac{4\rho_L}{\mu_L}\int_0^{\infty}\left\{\int_0^{\hat{h}_s} u(y)dy\right\}\tilde{f}_{\hat{h}_s}(h_s)dh_s \quad (25)$$

With values of $\tilde{f}_{h_s}(h_s)$ obtained as discussed above, it is possible to calculate the expected value of the substrate Reynolds number. Figure 12 shows the relationship between this calculated value of $\langle Re_s\rangle$ and the input Reynolds number Re_L in the absence of gas flow. It is now clear that even at very substantial total liquid flow rates the flow in the substrate is small. Considering that the adjacent wall or a gas phase is exposed to this substrate 30 to 50% of the time (Figure 11) it is clear that this small flow in the substrate will be important to the calculation of any transfer process.

A Theory for the Average Substrate Thickness. The large waves which move across the substrate have peak heights which are 6 to 10 times the average substrate thickness. Figure 12 shows that the liquid carried in these large waves is 10 to 20 times that flowing in the substrate. The large waves move with a velocity which is large compared to that of velocities in the substrate film. We speculate that this situation makes it possible to consider the large wave in front of a substrate as an effectively infinite reservoir of liquid and that the substrate film is formed by a process equivalent to the process of drainage when a plate is withdrawn from such a reservoir. The equivalence is illustrated in Figure 13. The actual situation is at the left. We hypothesize that the observed thickness $\langle h_s\rangle$ is the same as if a plate would be withdrawn from an infinite pool of liquid at a velocity equal to the celerity of the large waves c_w. This is shown at the right.

The theory of plate drainage and withdrawal is well developed (Levich, 1962; Groenveld, 1971, 1970; White and Tallmadge, 1965) for laminar films. White and Tallmadge (1965) have obtained a solution with few restrictions.

$$\frac{T_0 - \frac{1}{3}T_0^3}{(1-T_0^2)^{2/3}} = 0.944\ Ca^{1/6} \quad (26)$$

where for this application

$$T_0 = \langle h_s\rangle\left[\frac{\rho g_L}{\mu c_w}\right]^{1/2}$$

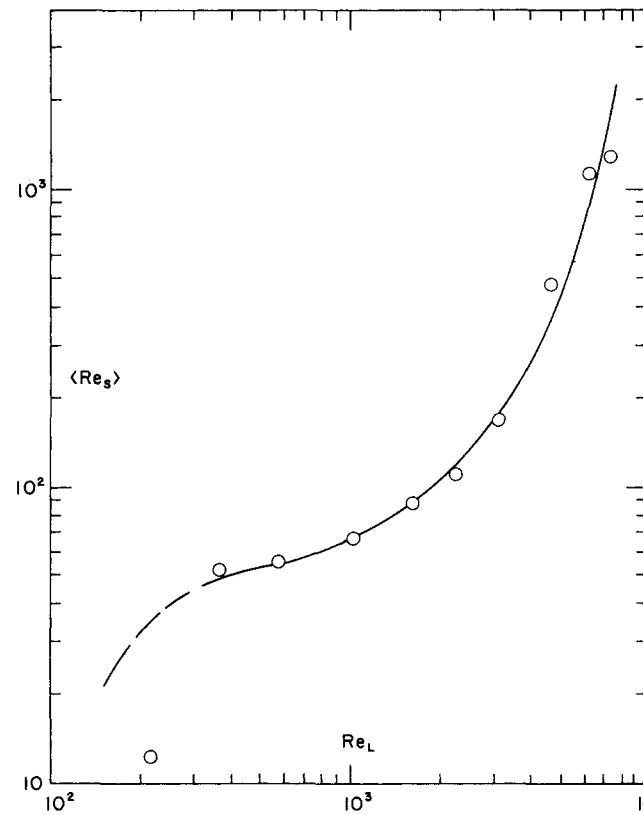

Fig. 12. Variation of average flow in substrate with input flow: zero gas rate.

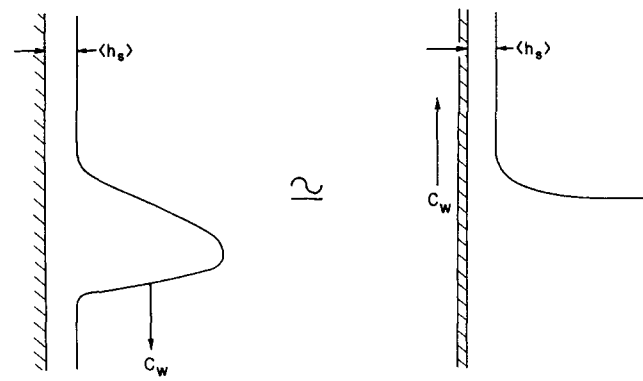

Fig. 13. Model for draining plate.

$$Ca = \frac{\mu c_w}{\sigma g_c}$$

Equation (26) will not apply for large values of Ca or for high rates when the film is partially in turbulent motion. A comparison of the experimentally measured $\langle h_s \rangle$ at no gas flow with those predicted by Equation (26) appears in Figure 14. The agreement is within measuring accuracy up to input Reynolds numbers of 4 to 5,000. Above this value the substrate Reynolds number exceeds 400 (see Figure 12) and it has been shown (Dukler, 1959) that film turbulence can be expected to be significant above a Reynolds number of about 300. An extension of this theory to turbulent film and for the case of concurrent gas flow will be presented in a paper to follow.

Structure of Waves on the Substrate

Typical data for substrate wave structure is shown here. Information in detail has been presented by Chu (1973).

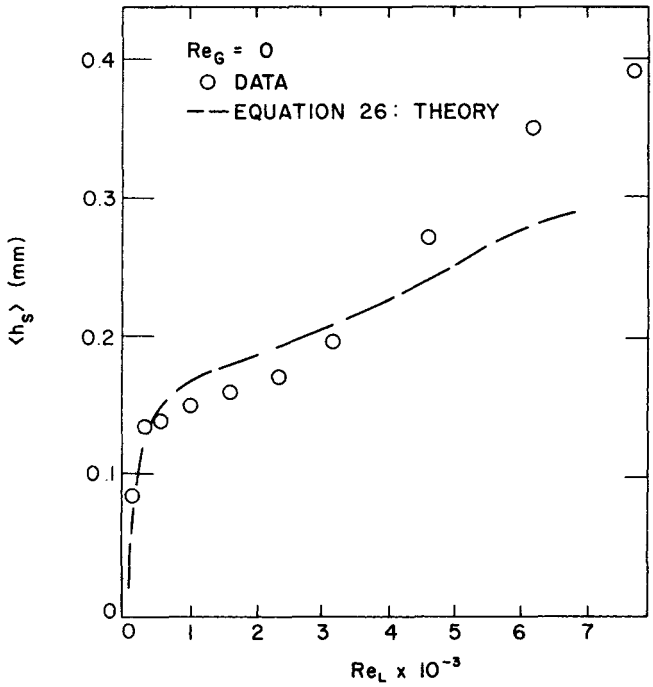

Fig. 14. Comparison of theory and experiment for substrate thickness.

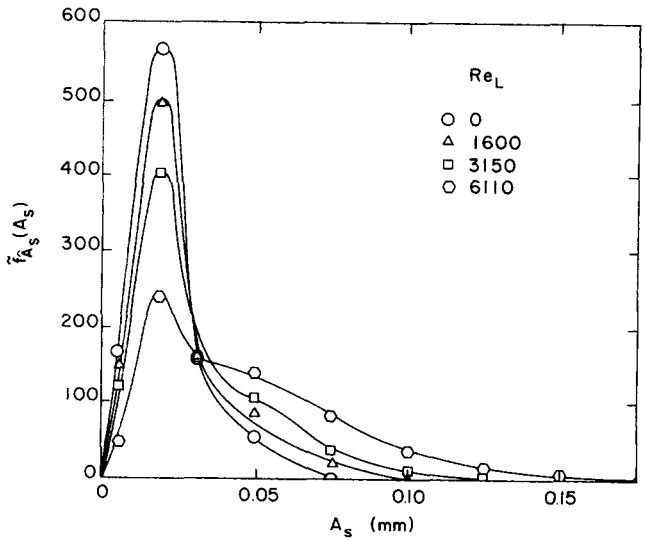

Fig. 15. Probability density of substrate wave amplitude: zero gas rate.

Extensive theoretical work has been reported which attempts to predict the properties of waves on films moving at low Reynolds numbers. These have been critically reviewed by Dukler (1972). The data of this study on the structure of substrate waves now make it possible to make definitive tests of these theories. For the substrate, certain key requirements of the theories are satisfied; namely, low flow rates, small wave amplitudes compared to wave length and low ratios of wave amplitude to average film thickness. As will be seen, these theories do not predict the observed wave properties.

Wave Amplitude, A_s. Probability densities of wave amplitude $f_{\hat{A}_s}(A_s)$ for a range of liquid rates in the absence of gas flow are shown in Figure 15. Note that the location of the modal peak is remarkably constant being within $\pm$ 0.0128 mm for all liquid rates. Considering the fact that the mean substrate thickness varies by a factor of four over this same range of flows strongly suggests that the waves which are formed are all of the same amplitude and that a process of dispersion or coalescence generates waves of other sizes, this process increasing as the flow rate increases.

The insensitivity of the amplitude of substrate waves to interfacial shear is clear from the data in Figure 16. Note that while the wave amplitude is insensitive to gas flow, the average substrate film thickness is not (see Figure 10), a rather unexpected result.

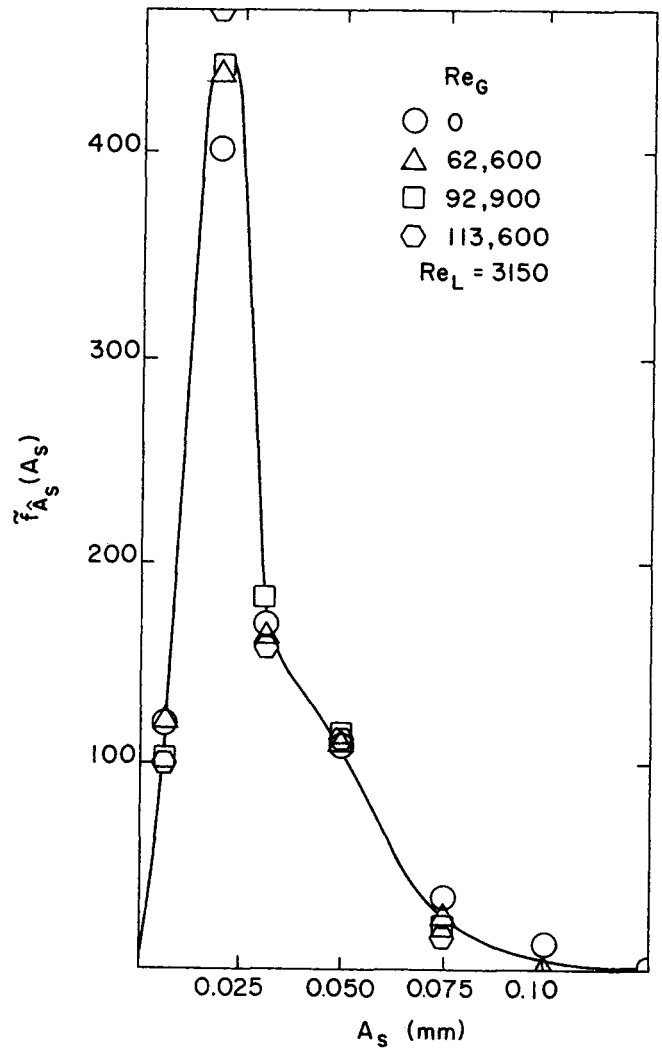

Fig. 16. Probability density of substrate wave amplitude: effect of gas rate.

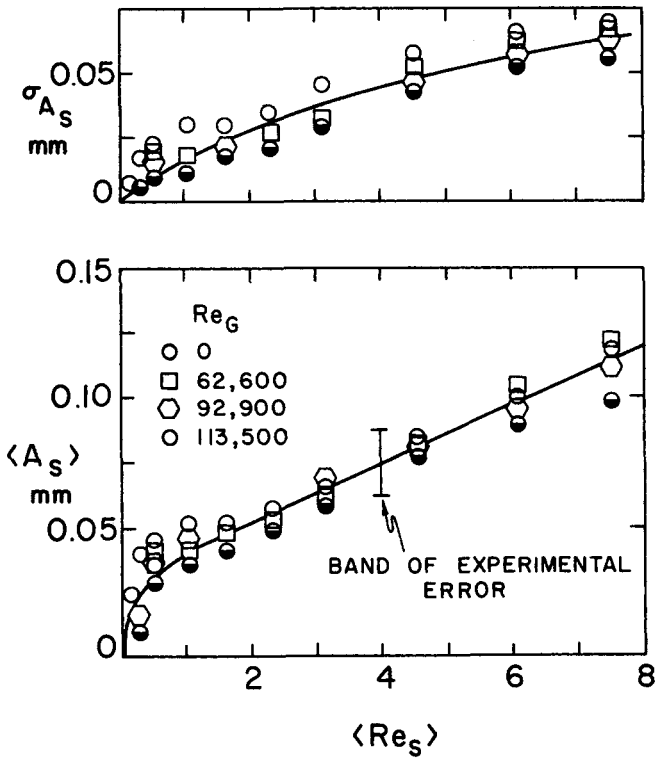

Fig. 17. Average and standard deviation of substrate wave amplitude.

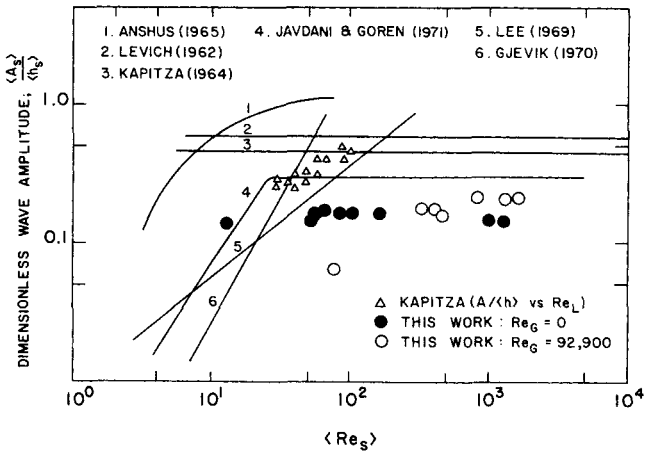

Fig. 18. Comparison of theory and experiment: substrate wave amplitude.

Values of $\langle A_s \rangle$ and σ_{A_s} appear in Figure 17. Comparison with data on the variance of h_{min} and h_{max} shows that the waves are quite uniform in size and that the variation in film thickness is due principally to the variation in the thickness of the film at the trough of the wave.

The dimensionless mean amplitude of substrate waves as measured here is compared with the prediction of six theories in Figure 18. Also included are the data of Kapitza (1964), but in this case it is important to note that his data include all wave amplitudes measured, not just those on the substrate and Re_L is the input Reynolds number. The theory with closest agreement, that of Javdani and Goren (1971), deviates from the data by at least a factor of two. A careful reexamination of that theory failed to disclose any numerical error.

Evidence of the marked difference between properties of the large waves and these substrate waves can be seen from a comparison of dimensionless amplitudes at similar Reynolds numbers.

$\langle Re_s \rangle$	$\langle A_s \rangle / \langle h_s \rangle$	Re_L	$A_w/\langle h \rangle$
165	0.16	210	0.37
470	0.16	570	0.58
1010	0.15	1015	0.95

Thus, at the same flow rate, waves on the substrate are smaller than the disturbance waves on the film by factors of 2 to 6.

Wave Base Time, T_{bs}. The probability density for T_{bs} and its dependence on gas and liquid rate is shown in Figures 19 and 20. Again the insensitivity of this small wave structure to gas flow is emphasized as is the suggestion of the dominance of a single wave size and shape.

The frequency of these small waves can be found from

$$f_s = \frac{1}{\langle T_{bs} \rangle} \tag{27}$$

Many theories have purported to predict these wave frequencies and these attempts are compared with experiment in Figure 21. Also shown are the data of Kapitza (1964) which reflects his counting of all waves on the surface, not just small waves. However, at the very low flow rates of Kapitza's experiments the number of large waves are few and frequency count would not be significantly distorted. Note that except for the Berbente and Ruckenstein (1968) attempt, all theories are poor predictors. However, the apparent good agreement of Berbente and Ruckenstein is, in fact, due to their use of Kapitza's data to evaluate certain constants in their model.

Velocity of Substrate Waves. Theories which predict the wave velocity usually show that the ratio of the velocity to the mean film thickness depends on the Reynolds number. The existence of two classes of waves suggests that the velocity of the large waves be normalized by the average thickness of the film and this ratio be compared with

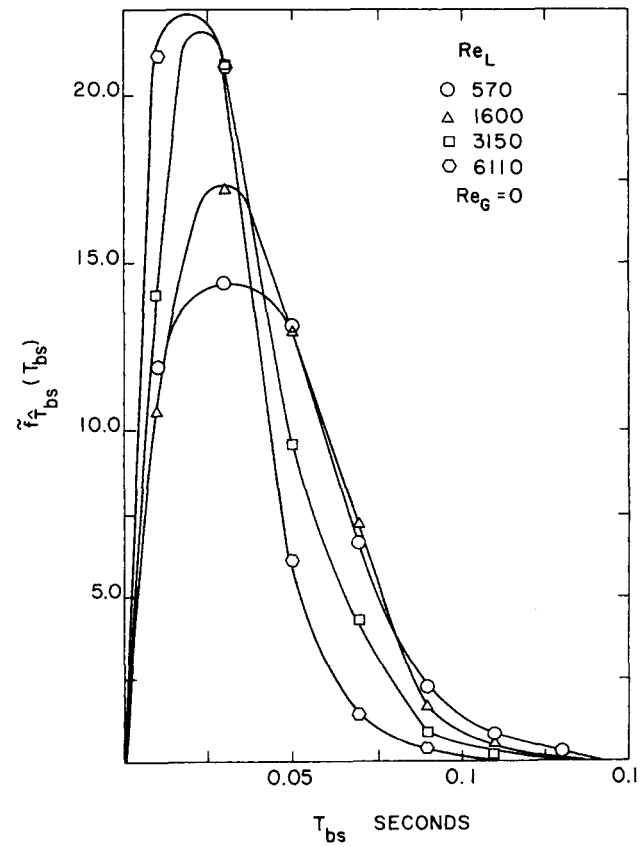

Fig. 19. Probability density of substrate wave base dimension: zero gas rate.

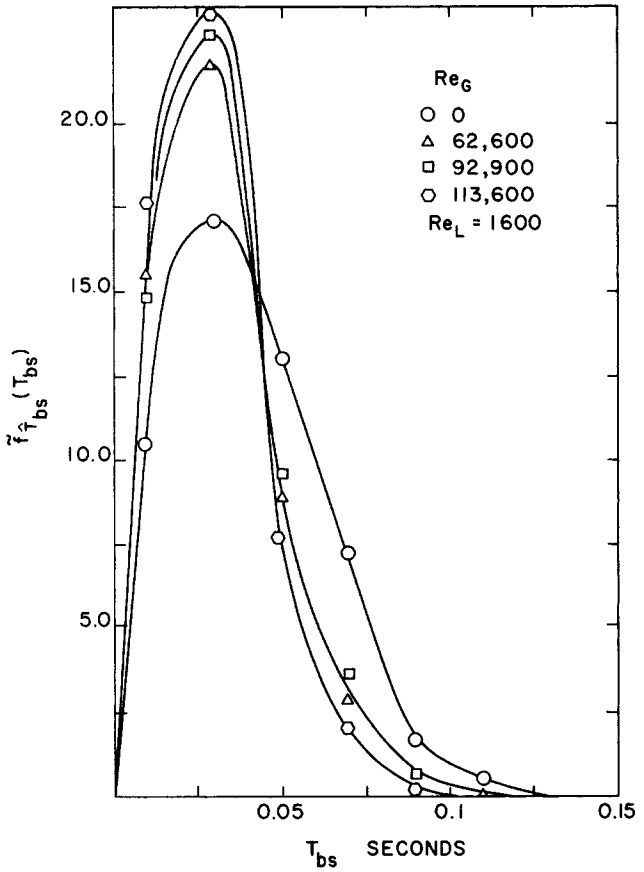

Fig. 20. Probability density of small wave base dimension: effect of gas rate.

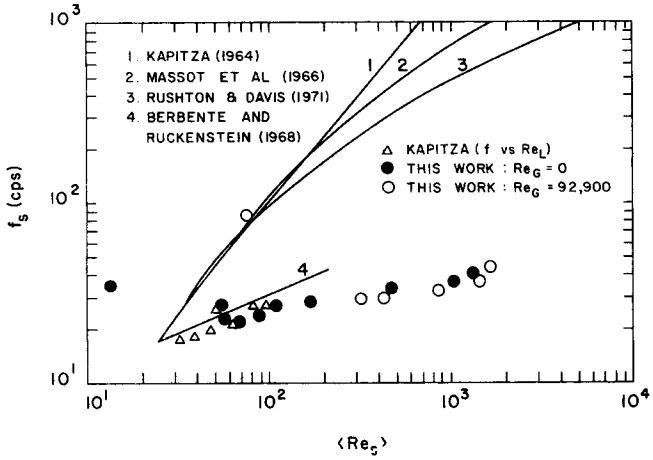

Fig. 21. Comparison of theory and experiment: substrate wave frequency.

Re_L. For the substrate the correlation should be between the ratio of the wave velocity to the velocity of the substrate film, $c_s/\langle u_s\rangle$, and the substrate Reynolds number. $\langle u_s\rangle$ is calculated from

$$\langle u_s\rangle = \frac{\nu}{4}\,\frac{\langle Re_s\rangle}{\langle h_s\rangle} \tag{28}$$

Figure 22 compares experimental data with and without gas flow with four theories. Also included are the data of Kapitza. It should be noted that his wave velocity represented the average of large and small waves. It is clear that no theory does an acceptable job of predicting the true situation. The fact that $c_s/\langle u_s\rangle$ is greater than 3.0 is surprising, but a careful recomputation of the data attest to their validity.

Wave Length. The wave length of substrate waves can be calculated from

$$\lambda_s = c_s\,\langle T_{bs}\rangle \tag{29}$$

The dimensionless wave length

$$N_{\lambda_s} = \frac{\lambda_s}{2\pi}\,\frac{g_L\rho}{g_c\sigma} \tag{30}$$

is plotted against the Weber number of the substrate,

$$N_{We} = \frac{\langle u_s\rangle\langle h_s\rangle}{\sigma} \tag{31}$$

in Figure 23 where it is compared with the prediction of five theories. None are satisfactory.

While substrate waves satisfy the condition required for existing theories (small wave amplitude and small slope), the theories do a poor job of predicting the properties of these waves. Part of the reason becomes clear from Figure 24 which describes the skewness of these substrate waves as measured by the ratio of the length (or passage time) of the front and the back of the wave. It would appear that these small substrate waves rapidly become nonsymmetrical during their growth process. Few of the existing theories consider more than the first harmonic in a Fourier series expansion of the wave shape. Several consider two terms and only one considers three. But in order to describe a wave with this degree of asymmetry, many more terms are required: Adding more terms in all published methods would make the mechanics of solution hopelessly complex. Thus, other types of orthogonal expansions will be needed to allow a description of the waves with fewer terms.

ACKNOWLEDGMENT

This work was supported by a grant from the U.S. Department of Interior, Office of Saline Water.

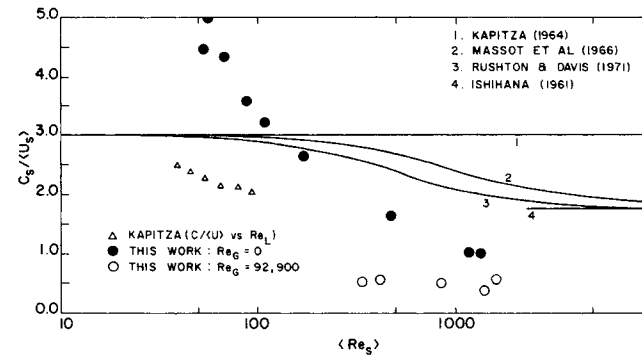

Fig. 22. Comparison of theory and experiment: velocity of substrate waves.

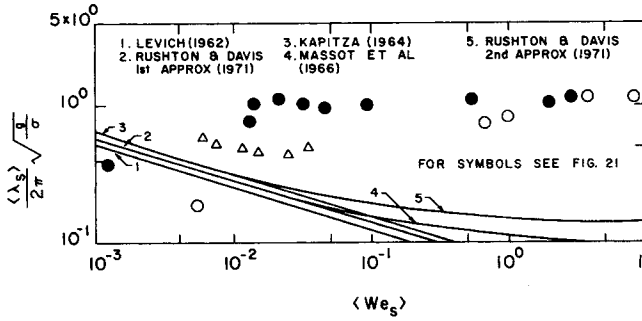

Fig. 23. Comparison of theory and experiment: substrate wave length.

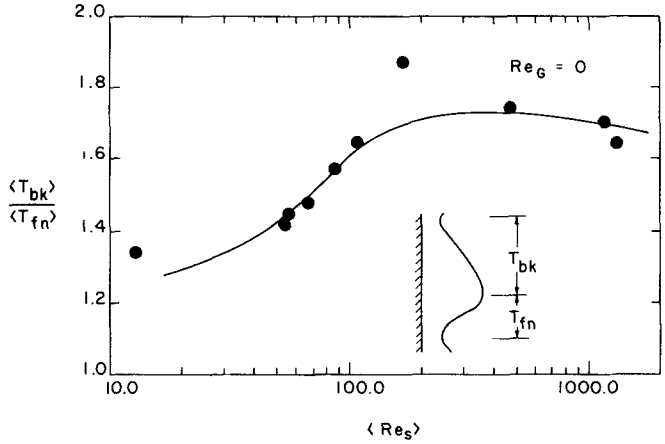

Fig. 24. Ratio of front-to-back dimension of substrate waves.

NOTATION

A = wave amplitude
A_s = wave amplitude of small waves
A_w = wave amplitude of large waves
a_j = coefficient of Fourier series
b_j = coefficient of Fourier series
c = wave velocity
c_s = velocity of small waves
c_w = velocity of large waves
c_a = dimensionless quantity $\mu_L\ c_w/\sigma g_c$
$\tilde{CV}_s$ = portion of $\tilde{f}\hat{h}(h)$ related to substrate
$\tilde{CV}_w$ = portion of $\tilde{f}\hat{h}(h)$ related to large wave
D = pipe diameter
F_s = time fraction of substrate
F_w = time fraction of large waves
f = frequency in cps
f_D = digitizing frequency
f_s = frequency of small wave
$\tilde{f}$ = probability density function
g_c = conversion constant
g_L = acceleration of gravity
h = film thickness
h_{max} = film thickness at the crest of the wave
h_{min} = film thickness at the trough in the front of the wave
h'_{min} = film thickness at the trough in back of the wave
h_s = substrate film thickness
h_w = film thickness of large waves
l = separation distance between probes
N_s = number of small waves in sample
N_w = number of large waves in sample
N_λ = dimensionless wave length, $\frac{\lambda}{2\pi}\frac{g_L\rho_L}{g_c\sigma}$
N_{We} = Weber number, uh/σ
$\tilde{Q}$ = quadrature-spectrum
Re_L = input Reynolds number
Re_s = substrate Reynolds number
$\tilde{S}$ = spectrum function
T = wave period
T_0 = dimensionless quantity, $\langle h \rangle\ (\rho_L\ g_L/\mu_L c_w)^{1/2}$
T_{bs} = time for passage of base of wave
T_{fn} = time for passage of front of wave
T_{bk} = time for passage of the back of the wave
T_{sep} = wave separation time
u = velocity in x direction
u_s = substrate velocity in x direction
W_L = mass flow rate of liquid
x = coordinate direction
y = coordinate direction

Greek Letters

$\tilde{\theta}$ = phase spectrum
$\tilde{\Lambda}$ = cospectrum
λ = wave length
μ_L = viscosity of liquid
ν = kinematic viscosity
ρ_L = density of liquid
σ = surface tension
ω = frequency in radian per sec.
$\langle\ \rangle$ = expected value
$\wedge$ = random number

LITERATURE CITED

Alves, G. E., "Cocurrent Gas Liquid Pipeline Contactors," *Chem. Eng. Progr.*, **66**, (7), 6 (1970).

Anshus, B. E., "Finite Amplitude Wavy Flow on a Thin Film on a Vertical Wall," Ph.D. dissertation, Univ. of Calif., Berkeley (1965).

Berbente, C. P. and E. Ruckenstein, "Hydrodynamics of Wavy Flow," *AIChE J.*, **14**, 774 (1968).

Chu, K. J., "Statistical Characterization and Modelling of Wavy Liquid Film in Vertical Two-Phase Flow," Ph.D. dissertation, Univ. of Houston, Texas (1973).

Dukler, A. E., "Characterization, Effects and Modelling of the Wavy Gas-Liquid Interface" in *Progress in Heat and Mass Transfer*, Pergamon, New York (1972).

———., "Dynamics of Vertical Falling Film Systems," *Chem. Eng. Progr.*, **55**, 62 (1959).

Gjevick, B., "Occurrence of Finite-Amplitude Surface Waves on Falling Liquid Film," *Phys. Fluids*, **13**, 1918 (1970).

Groenveld, P., "Drainage and Withdrawal of Liquid Films," *AIChE J.*, **17**, 489 (1971).

———., "High Capillary Number Withdrawal from Viscous Newtonian Liquids by Flat Plates," *Chem. Eng. Sci.*, **25**, 33 (1970).

Ishihara, T., Y. Iwagak, and Y. Iwasa, "Discussion on Roll Waves and Slug Flows in Inclined Open Channels," by Paul Mayer, *Trans. Am. Soc. Civil Eng.*, **126**, 548 (1961).

Javdani, K. and S. L. Goren, "Finite-Amplitude Wavy Flow on Thin Films," Intern. Symp. Two-phase System, Haifa, Israel (1971).

Kapitza, P. L., "Wave Flow of Thin Layers of a Viscous Fluid," Collected papers of P. L. Kapitza, MacMillan, New York (1964).

Lee, J., "Kapitza's Method of Film Flow Description," *Chem. Eng. Sci.*, **24**, 1309 (1969).

Levich, V. G., *Physiochemical Hydrodynamics*, pp. 674-692, Prentice-Hall, New Jersey (1962).

Massot, C., F. Irani, and E. N. Lightfoot, "Modified Description of Wave Motion in a Falling Film," *AIChE J.*, **12**, 445 (1966).

Nusselt, W., "Die oberflocaekondensation Des Wasserdampfer," *ZVDI*, **60**, 541 (1916).

Rushton, E., and G. A. Davis, "Linear Analysis of Liquid Film Flow," *AIChE J.*, **17**, 671 (1971).

Telles, A. S., "Liquid Film Characteristics in Vertical Two-phase Flow," Ph.D. dissertation, Univ. of Houston, Texas (1968).

———., and A. E. Dukler, "Statistical Characteristics of Thin, Vertical Wavy Liquid Films," *Ind. Eng. Chem. Fundamentals*, **9**, 412 (1970).

Webb, D., "Two-phase Flow Phenomena," Ph.D. dissertation, Univ. Cambridge (1970).

White, D. A. and J. A. Tallmadge, "Theory of Drainage of Liquids on Flat Plates," *Chem. Eng. Sci.*, **20**, 33 (1965).

Wicks, M., "Liquid Film Structure and Drop Size Distribution in Two-phase Flow," Ph.D. dissertation, Univ. of Houston, Texas (1967).

Manuscript received January 4, 1974; revision received March 28 and accepted April 5, 1974.